August 2010, Volume 7, No.8 (Serial No.69)
Journal of Communication and Computer, ISSN 1548-7709, USA

Simplified Texture Spectrum for Texture Analysis

Dong-Chen He[1] and Li Wang[2]

1. Department of Applied Geomatics, University of Sherbrooke, Sherbrooke, Qc. J1K 2R1, Canada

2. DLW Information Inc., 2578 Troyes, Sherbrooke, Qc. J1K 1W9, Canada

Received: May 10, 2010 / Accepted: June 01, 2010 / Published: August 25, 2010.

Abstract: The authors proposed the texture unit-based texture spectrum approach in 1990, which has been used for texture analysis, including texture characterization, texture classification, texture edge detection, and textural filtering. One of the most important disadvantages related to this method is the large number of texture units (6,561) and its redundancy. This paper aims at simplifying the original texture spectrum by reducing the 6,561 texture units into only 15 units without significant loss of discriminating power. Promising results are presented here via several experimental investigations over some of Brodatz's natural texture images.

Key words: Texture analysis, texture spectrum approach, texture classification, texture edge detection, texture difference measure, pattern recognition.

1. Introduction

Texture plays an important role in pattern recognition and image processing, particularly when the targeted objects have similar grey level distributions. In such cases, conventional individual pixel-based analysis methods are not efficient, while texture analysis can provide useful, complementary information. Sometimes, texture analysis is the only way to characterize object properties.

Statistical approaches are an important part of texture analysis, which proposes texture features based on some statistical properties of images. In 1973, Haralick [1] proposed the co-occurrence matrix method for textural information extraction, which is a typical statistical approach and has been widely used. For more than 30 years, these well-known co-occurrence matrices based 14 Haralick's statistics have been proven to be the most popular and most efficient texture features [2].The co-occurrence matrix method provides second-order statistics to generate texture features. A co-occurrence matrix element in the position of (i, j) represents the frequency or probability to finding a pair of pixels with a grey level from i to j and separated by a predefined displacement vector d. These features, however, represent only a part of the texture properties of the image with the given displacement vector d. Users can calculate several co-occurrence matrices in different directions, for example, 0°, 45°, 90°, and 135°. This could, however, present some drawbacks in practice. Firstly, the choice of this displacement vector d depends on experimental cases and the justification would be objective. Secondly, the resultant 14 texture features are often redundant and too numerous, particularly when using more displacement vectors.

In order to overcome these drawbacks, the authors [3] proposed, in 1990, the texture spectrum approach, based on texture units, which characterize local texture information in all eight directions. This method has been applied to texture feature extraction [4], texture classification [5], edge detection [6], and textural filtering [7]. The texture spectrum has been widely

Corresponding author: Dong-Chen He, Ph.D., professor, research fields: texture analysis, pattern recognition, digital image processing, geometrics and remote sensing. E-mail: Dong-Chen.He@Usherbrooke.ca.

Li Wang, Ph.D., senior research scientist, research fields: digital image processing, pattern recognition, geographical information systems and remote sensing.

mentioned and reported in the literature as well as in some textbooks [8-11]. One of the advantages of the texture spectrum approach is that the texture aspects of an image are characterized by the corresponding texture spectrum instead of a set of texture features and that the texture spectrum can be directly used for image classification and image analysis.

The initial studies [3-7] defined texture units as a central pixel with its neighboring pixels in all eight directions to form a 3×3 grid. The grey-level differences between the central pixel and its eight neighbors is simplified to three situations (<, =, and >). The texture spectrum is a simple histogram of all the texture units within a moving window. This texture spectrum, with a dimension of $3^8 = 6{,}561$, is the unique feature for characterizing the image's texture information. Recent studies [12] have reported that the calculations in eight directions are probably redundant and the texture spectrum defined in only four directions, 0°, 45°, 90°, and 135° can give similar discriminatory power, but with a reduced dimension of $3^4 = 81$.

Two major inconveniencies, however, still remain. Firstly, the dimension of 81 is still too large for convenient application. Comparing two texture spectrums should involve calculating the difference in each of 81 dimensions. This is similar to a data space of 81 image bands or channels. Secondly, all the possible texture units are ordered in a 3-tuple system, such that some similar textural situations could result in very different texture unit numbers, which equal $N_{TU} = \sum E_i \, 3^{i-1}$, with i = 1, 2, 3, and 4, respectively, for the four directions and with E_i = 0, 1, or 2, which corresponds, respectively, the situation of <, = and > between the central pixel and its neighboring pixels. Consequently, there still exists redundancy in this way of numbering texture units.

In this paper, we present a simplified texture spectrum approach, by eliminating the redundancy of the texture unit numbers, thereby reducing the texture spectrum dimension to 15. Section 2 describes the methodology, while section 3 investigates the discriminatory ability of the proposed method with some experimental results. Conclusions are presented in section 4.

2. Methodology

In this section, we will describe the basic principles used for estimating the texture spectrum (TS), including the texture unit (TU) and the texture unit number (N_{TU}).

2.1 Texture Unit (TU)

The texture unit (TU) is used for extracting the local texture information from a neighborhood of 3 × 3 pixels, which represents the smallest complete unit surrounding the central pixel in all eight directions. Recent studies [12] have reported that the calculations in eight directions are probably redundant and that only four directions (0°, 45°, 90°, and 135°) can be used without loss of discriminatory power.

Let us consider a neighborhood in Fig. 1 with only four directions (0°, 45°, 90°, and 135°), which can be noted as a set containing five elements: $\boldsymbol{V} = \{V_0, V_1, V_2, V_3, V_4\}$, where V_0 represents the grey-level value of the central pixel and V_i represents the grey-level value of the neighboring pixel i, with i = 1, 2, 3, 4. The key concept of the texture spectrum method is to use the relative intensity relations between pixels, instead of their absolute intensity values (such as the co-occurrence matrix), to represent the local texture aspect, which is more faithful to the texture characteristics. We can define the corresponding texture unit (TU) as a set containing four elements: TU = $\{E_1, E_2, E_3, E_4\}$, where E_i is determined by comparing the grey-level difference between the central pixel

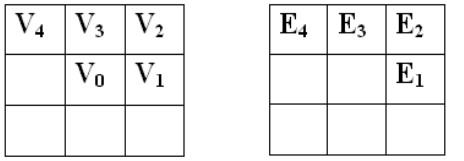

Fig. 1 Converting a neighborhood to texture unit.

and its four neighbors. We will simplify these difference relationships into three situations (=, < and >), which will be noted as 1, 2, and 6, respectively:

$$E_i = \begin{cases} 1 & \text{if } |V_0 - V_i| \le \Delta \\ 2 & \text{if } (V_i - V_0) > \Delta \\ 6 & \text{if } (V_0 - V_i) > \Delta \end{cases} \quad (1)$$

Where Δ represents a small positive value, which is influenced by the image noise and the image grey-level distribution. We simplify this choice in our experiments by first calculating a histogram of all the difference values $(V_0 - V_i)$ for the entire image to be analyzed and then assign the Δ value so that the histogram will be roughly divided into three equal proportions centered around the $(V_0 - V_i) = 0$ axis.

It should be noted that, generally, N different values can be defined for E_i instead of only three, as defined above. A large N value will reveal more details in the local texture, but requires much more calculation time. For N=3, as defined above, the combination of all four elements results in a total of $3^4 = 81$ possible texture units, whereas the total would be $5^4 = 625$ possible texture units when N=5 . It would be interesting to note that the commonly used co-occurrence matrix is the particular case of N= 256 (if the image is coded in 8 bits) with only two pixels considered: $256^2 = 65{,}536$ possible units for a co-occurrence matrix. On the other hand, our studies [12] have concluded that, for the same total number of texture units, it would be advantageous to take into account more pixels and reduce the N value. Our experiences show that using N=3 and four neighboring pixels represents a good compromise, which will result in a total of $3^4 = 81$ possible texture units. This is much less than the initial proposition of $3^8 = 6{,}561$ texture units.

2.2 Texture Unit Number (N_{TU})

These 81 texture units can be labeled and ordered in different ways. In our initial studies, each texture unit $TU = \{E_1, E_2, E_3, E_4\}$ was labeled with a 3-base number with $N_{TU} = \sum E_i \, 3^{i-1}$, for i = 1, 2, 3, and 4, respectively. In the present simplified approach, we do not distinguish the order of the four neighborhood pixels in labeling the texture unit number. This will group all the 81 texture units into only 15 possible situations (Table 1). In addition, we use the values of 1, 2, and 6 to represent three situations of the E_i values, so that the sum of these four elements will result in 15 unique no-redundancy values, which can be directly used as the texture unit number (N_{TU}), varied from 1 to 15 (except for 16, 19, 20, and 24).

Table 1 Labeling of texture units.

Combinations of Ei				Sum of Ei values	N_{TU}
1	6	6	6	19	1
2	6	6	6	20	2
6	6	6	6	24	3
1	1	1	1	4	4
1	1	1	2	5	5
1	1	2	2	6	6
1	2	2	2	7	7
2	2	2	2	8	8
1	1	1	6	9	9
1	1	2	6	10	10
1	2	2	6	11	11
2	2	2	6	12	12
2	2	6	6	16	13
1	1	6	6	14	14
1	2	6	6	15	15

The objective of this simplification and the labeling is (i) to reduce the texture spectrum dimension from 81 to 15, and (ii) to facilitate the labeling of the texture units by just summing the four elements of the texture unit (i.e. $\sum E_i$).

2.3 Texture Spectrum (TS)

Just like the grey-level value of a given pixel represents its spectral propriety, the texture unit, via the texture unit number N_{TU}, represents the textural aspect of the given pixel. The statistics of the occurrence frequency function of all the texture units in an image, or a moving window, should reveal the texture information for the image to be analyzed, in the same way that grey-level values of image pixels form an image histogram. Herein, we refer to this histogram of texture units as the texture spectrum, with the abscissa

indicating the texture unit number N_{TU} and the ordinate representing its occurrence frequency.

2.4 Texture Difference Measure (TDM)

Given a texture image A with a texture spectrum TS_A ={ $TS_A(1)$, $TS_A(2)$, …, $TS_A(15)$,} and a texture image B with a texture spectrum TS_B ={ $TS_B(1)$, $TS_B(2)$, …, $TS_B(15)$,}, where $TS_A(k)$ represents the occurrence frequency of the texture unit numbered k in the image A, we can use different methods to measure the difference between these two images.

First of all, we can use the Euclidian distance, also called the minimum distance:

$$TDM = SQRT\{[TS_A(1) - TS_B(1)]^2 + [TS_A(2) - TS_B(2)]^2 + \ldots, +[TS_A(15) - TS_B(15)]^2\} \quad (2)$$

Two similar texture images would result in a smaller TDM value, whereas a large TDM value would reveal more texture differences between the two images.

Since the occurrence frequency of the texture spectrum can be considered as a probability distribution, we can also use the well-established information theory to measure similarity between two texture spectrums. For example, Chang and Chen [11] suggested using the information divergence as the TDM. Other distance concepts may also be used as the TDM instead of Euclidian distance.

3. Experimental Results

In this section, the proposed simplified texture spectrum will be evaluated against some Brodatz's natural texture images [13]. Brodatz's textures are commonly used in pattern recognition and texture analysis for performance evaluation. This could facilitate the comparison between different approaches. Ours experiments were conducted:

(1) to measure the similarity within images with the same texture;

(2) to evaluate the discriminating power between different textures;

(3) to detect texture boundaries using simplified texture spectrum.

The minimum distance (Eq. (2)) was used as the texture difference measure (TDM).

3.1 Similarity within Same Textures

Eight Brodatz's textures were used in the first experiment. Each image is represented by 640 × 640 pixels coded in 8 bits per pixel. They are, respectively, images D4, D16, D49, D55, D57, D77, D82, and D105. These eight textures are presented in Fig. 2, with their emplacement indicated by Fig. 3. For each parent texture image of 640 × 640 pixels, 100 independent daughter images were extracted without any overlap

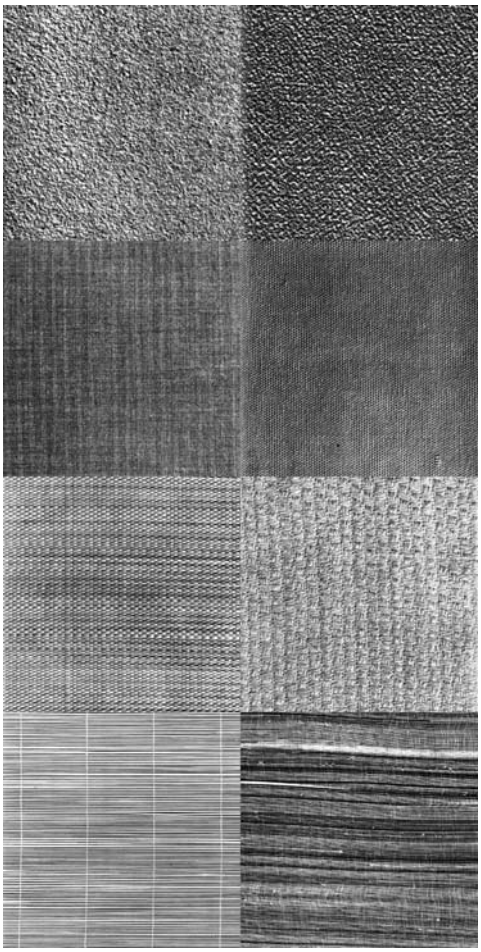

Fig. 2 Brodatz's textures for the 1st evaluation.

D4	D57
D16	D77
D55	D82
D49	D105

Fig. 3 Emplacement of the 8 textures of Fig. 2.

Table 2(a) Averaged TDM between parent and daughter textures.

Size	D4	D16	D49	D55	D57	D77	D82	D105
9×9	0.116	0.023	0.174	0.114	0.117	0.104	0.132	0.122
11×11	0.097	0.019	0.127	0.090	0.096	0.088	0.112	0.112
13×13	0.083	0.021	0.126	0.086	0.082	0.069	0.101	0.096
15×15	0.072	0.016	0.116	0.076	0.070	0.062	0.094	0.089
17×17	0.064	0.017	0.082	0.064	0.060	0.057	0.082	0.075
19×19	0.059	0.013	0.073	0.057	0.054	0.049	0.076	0.070
21×21	0.053	0.012	0.074	0.055	0.050	0.043	0.065	0.069
23×23	0.047	0.013	0.069	0.051	0.045	0.042	0.059	0.063
25×25	0.043	0.012	0.088	0.047	0.039	0.039	0.054	0.056
27×27	0.041	0.010	0.085	0.044	0.039	0.035	0.048	0.056
29×29	0.040	0.011	0.064	0.041	0.037	0.033	0.047	0.051
31×31	0.038	0.010	0.062	0.037	0.035	0.034	0.039	0.050
33×33	0.035	0.010	0.062	0.036	0.033	0.029	0.039	0.046
35×35	0.033	0.010	0.070	0.035	0.033	0.028	0.036	0.047
37×37	0.032	0.010	0.066	0.036	0.029	0.027	0.035	0.043
39×39	0.030	0.009	0.056	0.030	0.028	0.026	0.032	0.043
41×41	0.030	0.010	0.057	0.028	0.028	0.025	0.031	0.041
43×43	0.028	0.011	0.056	0.027	0.026	0.024	0.032	0.040
45×45	0.027	0.007	0.057	0.028	0.025	0.023	0.030	0.040
47×47	0.024	0.009	0.060	0.025	0.024	0.021	0.029	0.039
49×49	0.022	0.008	0.055	0.026	0.023	0.021	0.028	0.037
51×51	0.022	0.009	0.055	0.024	0.023	0.021	0.027	0.036
53×53	0.022	0.008	0.053	0.024	0.020	0.020	0.026	0.035
55×55	0.019	0.007	0.057	0.022	0.019	0.019	0.025	0.035
59×59	0.019	0.009	0.057	0.020	0.019	0.017	0.025	0.035

Table 2(b) Standard derivations of TDM between parent and daughter textures.

Size	D4	D16	D49	D55	D57	D77	D82	D105
9×9	0.026	0.103	0.076	0.023	0.028	0.022	0.039	0.046
11×11	0.022	0.087	0.066	0.023	0.022	0.020	0.036	0.038
13×13	0.015	0.078	0.051	0.021	0.018	0.014	0.034	0.034
15×15	0.015	0.068	0.043	0.021	0.016	0.012	0.029	0.041
17×17	0.015	0.064	0.050	0.016	0.012	0.012	0.025	0.032
19×19	0.012	0.059	0.039	0.012	0.013	0.010	0.019	0.026
21×21	0.012	0.054	0.034	0.015	0.013	0.009	0.015	0.031
23×23	0.011	0.050	0.030	0.012	0.010	0.008	0.013	0.030
25×25	0.010	0.046	0.027	0.013	0.010	0.007	0.014	0.025
27×27	0.007	0.041	0.026	0.013	0.009	0.008	0.009	0.023
29×29	0.010	0.041	0.031	0.010	0.009	0.009	0.011	0.020
31×31	0.009	0.039	0.028	0.007	0.010	0.007	0.007	0.017
33×33	0.008	0.036	0.027	0.008	0.009	0.004	0.008	0.017
35×35	0.009	0.035	0.027	0.008	0.008	0.006	0.005	0.017
37×37	0.009	0.031	0.029	0.007	0.008	0.007	0.007	0.018
39×39	0.008	0.031	0.025	0.005	0.008	0.003	0.006	0.019
41×41	0.008	0.031	0.024	0.006	0.006	0.004	0.007	0.020
43×43	0.008	0.029	0.026	0.005	0.006	0.003	0.006	0.020
45×45	0.008	0.029	0.021	0.005	0.006	0.004	0.006	0.020

(to be continued)

47×47	0.005	0.028	0.021	0.004	0.006	0.004	0.005	0.019
49×49	0.005	0.026	0.028	0.005	0.005	0.003	0.005	0.017
51×51	0.007	0.025	0.025	0.005	0.005	0.003	0.005	0.014
53×53	0.007	0.025	0.024	0.005	0.006	0.003	0.004	0.013
55×55	0.007	0.023	0.022	0.006	0.004	0.004	0.003	0.014
59×59	0.005	0.023	0.024	0.007	0.005	0.003	0.002	0.014

for each size of 9 × 9, 11 × 11, … and 59 × 59 pixels. We then calculated the average distance between the parent image and each daughter image using the minimum distance TDM. This is to evaluate the consistence ability of the texture spectrum within the same textures. Table 2(a) (averaged TDM) and Table 2(b) (standard derivation of TDM) show the experimental results for the eight texture images of Fig. 2.

Table 2(a) and Table 2(b) show that the distances between the parent and daughter texture images are relatively small and consistent, demonstrating the similarity within images having the same texture. It could also be noted that this similarity decreases as does the size of the daughter textures, particularly for coarse textures. This can also help us in selecting an appro- priate window size in texture image classification.

3.2 Discriminating between Different Textures

In order to evaluate the discriminating ability of the simplified texture spectrum, we first calculated the Euclidian distance TDM between the eight parent textures; the results are presented in Table 3. From Table 3, we can note that these distances vary from 0.040 to 0.503. The texture D49 is quite different from all the other images, followed by texture D105. Texture D4, on the other hand, is quite similar to texture D57.

One of the advantages of the texture spectrum approach is that the TDM can be used directly to classify texture images, instead of a set of features. A supervised approach was used to perform this classification with the eight textures in Fig. 2. A small sample (approximately 50 × 50 pixels) has been collected at the center of each texture. Then, the whole image in Fig. 2 was classified by a moving window of 31 × 31 pixels, using the minimum distance rule. At a given position of the moving window, we calculate the TDM value between the moving window and each of the eight texture samples. Then, we assign the central pixel of the moving window to the class that represents the minimum TDM value.

Fig. 4 shows the classification result, where the borders have not been processed due to the moving window size. A visual comparison of Fig. 2 and Fig. 4 shows that the eight textures are relatively well classified except for the regions near the texture boundaries.

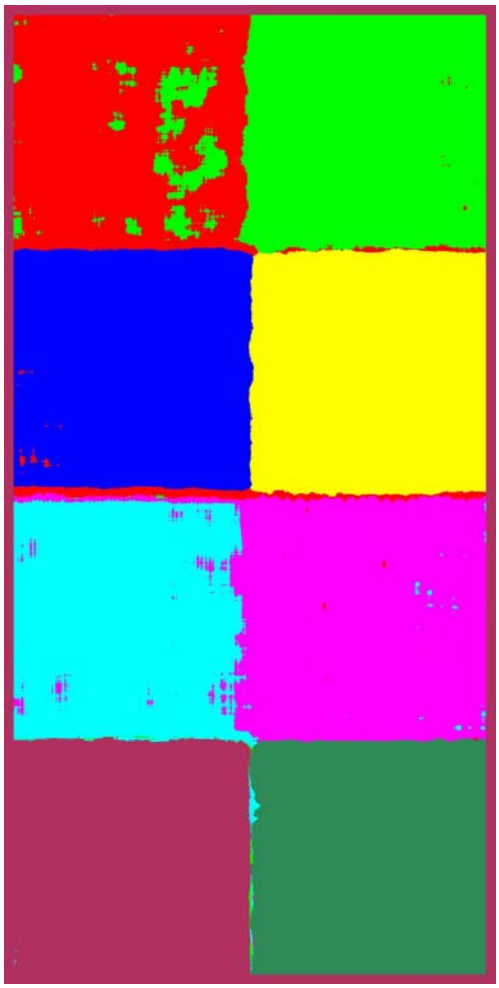

Fig. 4 Classification of Fig. 2 using texture spectrum.

Table 3 TDM values between 8 textures of Fig. 2.

	D4	D16	D49	D55	D57	D77	D82
D4	0						
D16	0.100	0					
D49	0.453	0.503	0				
D55	0.099	0.184	0.382	0			
D57	0.040	0.122	0.441	0.087	0		
D77	0.102	0.092	0.489	0.156	0.111	0	
D82	0.066	0.148	0.400	0.051	0.066	0.129	0
D105	0.157	0.159	0.413	0.176	0.167	0.195	0.164

Table 4 Confusion matrix for Fig.4 (in %).

Classified	Texture images (truth)							
	D4	D57	D16	D77	D55	D82	D49	D105
D4	87.11	0.71	2.89	0.95	0.94	1.61	0.00	0.00
D57	12.73	99.28	0.00	0.14	0.18	0.00	0.06	0.30
D16	0.15	0.00	97.06	0.49	0.00	0.00	0.00	0.00
D77	0.00	0.02	0.02	98.42	0.00	0.07	0.00	0.00
D55	0.00	0.00	0.00	0.00	90.06	0.40	0.26	0.59
D82	0.00	0.00	0.03	0.00	8.67	97.90	0.00	0.44
D49	0.00	0.00	0.00	0.00	0.16	0.00	99.67	0.09
D105	0.00	0.00	0.00	0.00	0.00	0.03	0.02	98.58

At these boundaries, the moving window crosses two kinds of different textures, resulting in a mixed spectrum, thereby lowering classification accuracy. It is interesting to compare this classification with the distance table in Table 3. Fig. 4 reveals that texture D49 is quite distinct from all the other textures, followed by textures D105 and D77. Table 3 shows exactly the same conclusion with the highest distance values for texture D49 from all the others, followed by textures D105 and D77. Inversely, Fig. 4 shows the most confusion between textures D4 and D57, followed by between D55 and D82, while Table 3 gives the lowest value (0.040) between D4 and D57, followed by 0.051 between D55 and D82. These observations coincide with the visual interpretation of Fig. 2.

This visual analysis of the classification results was accompanied by quantitative statistics presented in a confusion matrix (Table 4). It yields conclusions similar to the above analysis, that is, the greatest confusion occurred from D4 to D57, and for D55 to D82, while the best classification accuracy was achieved for D49, D105, and D77 with 99.67%, 98.58%, and 98.42% of correct classification rates, respectively. The average correct classification rate for the whole image is 96%, with a corresponding Kappa coefficient of 0.95.

When compared to the original texture spectrum (with 6,561 texture units) used for texture classification [5], the simplified texture spectrum yields similar classification accuracy, but with a much reduced data dimension and calculation requirement. It can be easily used in practice for processing a large volume of data.

In addition, we carried out the same classification procedure for the eight textures in Fig. 2 using some common co-occurrence matrix based texture features: Mean, Variance, Homogeneity, Contrast, Dissimilarity, Entropy, Second Moment, and Correlation. Using the same samples and the same minimum distance rule, we obtained the classification results presented in Fig. 5. Obviously, there is much more confusion between D4 and D57, between D16 and D77, and between D55 and D82.

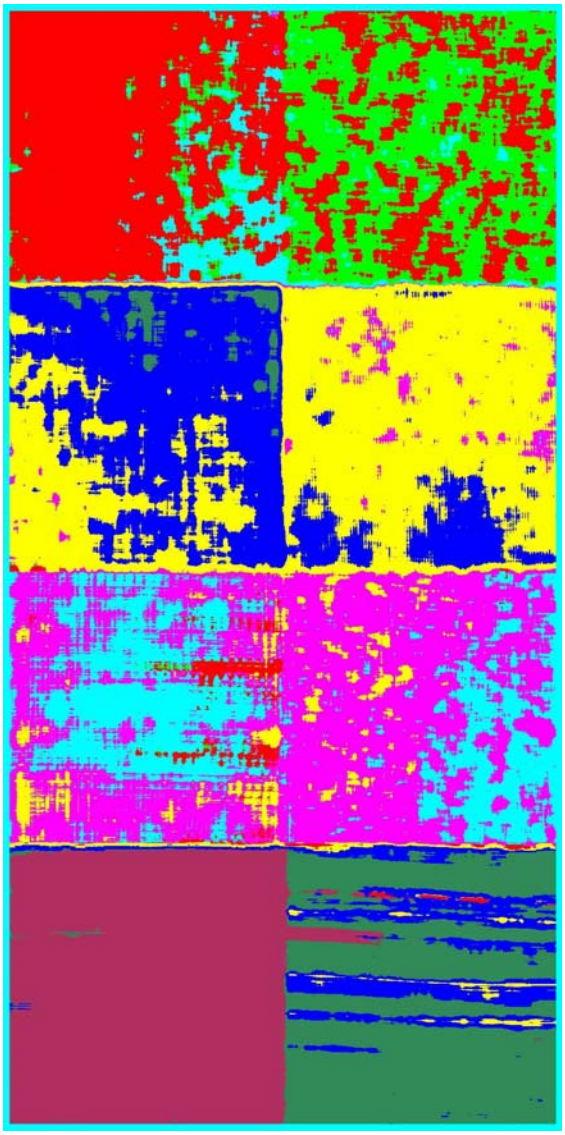

Fig. 5 Classification result of Fig. 2 using co-occurrence matrix based features.

To further evaluate the proposed approach, we removed the two last textures (D49 and D105) from Fig. 2 and added two more similar textures (D24 and D29) to the configuration, with different geometric forms (Fig. 6). The corresponding classification results are presented in Fig. 7. We can conclude that the eight textures are relatively well classified.

3.3 Texture Boundary Detection

Edge detection plays an important part in research into pattern recognition, image processing, and computer vision. Often, it constitutes the first step in many

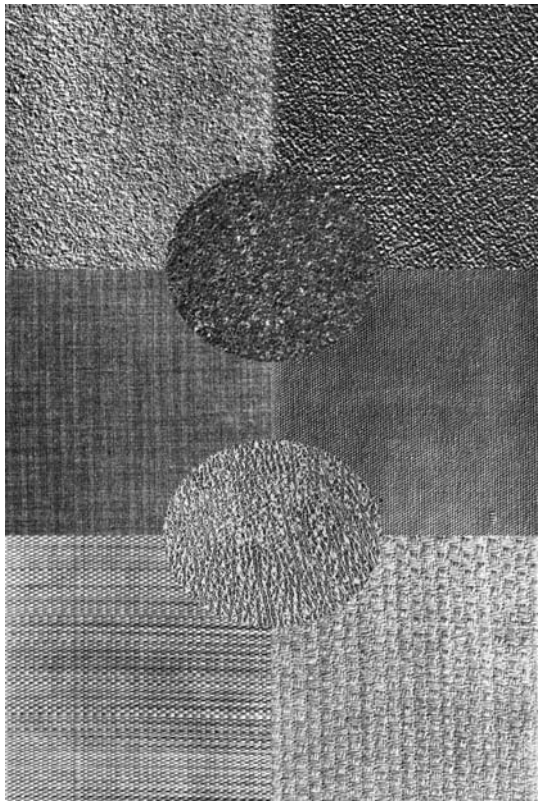

Fig. 6 Brodatz's textures for 2nd evaluation.

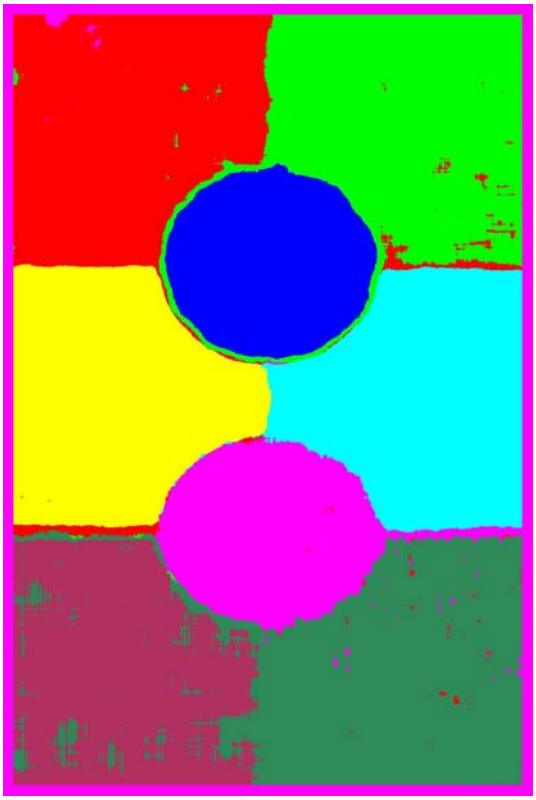

Fig. 7 Classification of Fig.6 using the simplified texture spectrum.

image analysis applications, such as image segmentation, feature or object extraction, etc. The goal of edge detection is to locate regions at which pixel intensity changes sharply.

Traditional edge detection methods can be grouped into two categories: 1st derivative and 2nd derivative [14]. Operators, such as the Roberts, Sobel, Prewitt, and Canny methods, are typical 1st derivative edge detection operators, which calculate the intensity gradient of the original image. In contrast, Gaussian-Laplacian and Marr-Hildreth edge detection are typical 2nd derivative based methods, which apply zero-crossings of second-order derivatives to identify the rate of change in the intensity gradient. These edge detection operators are widely used in practice, with the basic assumption that pixel intensity is more or less constant within regions and will change sharply at the boundary regions. Yet they are unable to locate textured region boundaries due to the intrinsic texture micro-edges within regions. The 1st and 2nd derivatives will respond strongly to the micro-edges within texture regions. One possible solution would be to replace the intensity values of the edge detectors with texture measures that can efficiently characterize texture regions.

Our experiment consists in combining traditional edge detection techniques with the texture spectrum. In other words, pixel intensity values in edge detection operators are replaced with the simplified texture spectrum.

Fig. 8 presents eight of Brodatz's textures used in this experiment. They are, respectively, images D4, D16, D24, D29, D55, D57, D77, and D82. Each texture has 640 × 640 pixels coded in 8 bits. These textures constitute some horizontal and vertical straight lines and two circles, which may represent most of the complex situations encountered in natural images. In addition, each texture has been stretched with the same histogram matching, resulting in very similar visual appearances. In some cases, it might be very difficult to distinguish the texture boundaries even with human

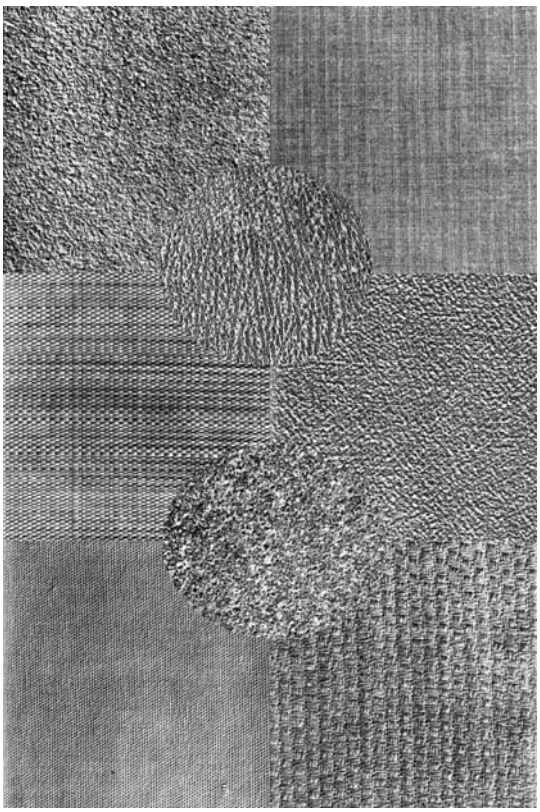

Fig. 8 Brodatz's textures used for 3rd evaluation.

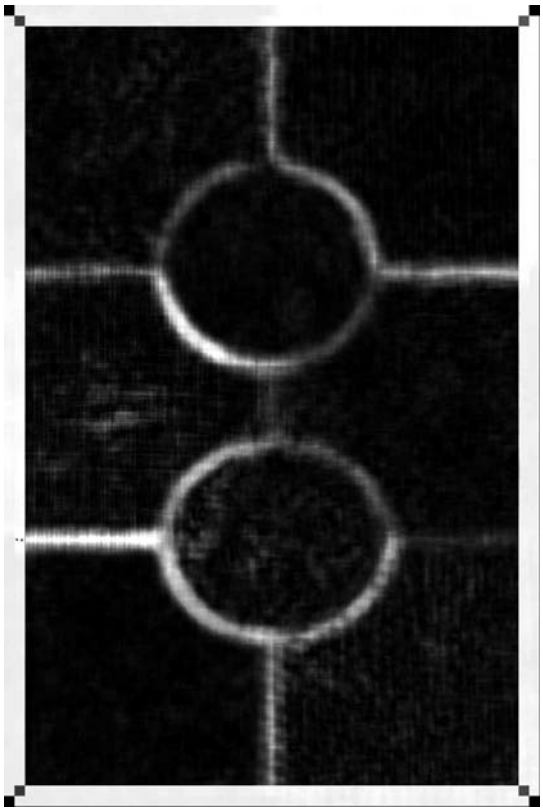

Fig. 9 Texture boundaries detected from Fig. 8.

interpretation. Fig. 9 shows the edge detection results using the Roberts operator and the simplified texture spectrum. In other words, the pixel intensity difference between two diagonal positions in the Roberts operator is replaced with the texture difference measure (TDM) from Eq. (2).

These results reveal that the proposed method can effectively extract the texture boundaries between textures and ignore the micro-edges within texture regions. It should be noted that the four exterior boundaries were not processed due to the geometric effect of the moving window and that post-processing may improve the resultant boundaries.

4. Conclusions

This paper presented a simplified texture spectrum for texture analysis. The proposed approach eliminates the redundancy of the texture unit numbers, which reduces the texture spectrum dimension from 6,561 to 15. Such a simplified method can be applied more easily in practice to classify texture images, instead of resorting to a set of complex features that are often redundant and too numerous. Several experimental examples indicate the promising performance of the proposed method in classifying texture images and in detecting texture boundaries. Compared with the initial texture spectrum, the simplified texture spectrum can yield the same discriminating performance, but with much less data dimension and calculation requirements.

This research seems to provide additional confirmation of our previous study [12], with the conclusion that it would be better to use more vectors for characterizing the local texture aspects than only one pair of pixels as with co-occurrence matrix based approaches. The texture discriminating measure (TDM) proposed in this paper seems to be a good indicator for measuring the similarity degrees between texture images. It provides lower values within the same textures and results in larger values for different textures.

Acknowledgments

The authors of this paper are grateful to the Natural Sciences and Engineering Research Council (NSERC) of Canada for sponsoring this research through the discovery grant awarded to Dong-Chen He.

References

[1] R.M. Haralick, K. Shanmugam, I. Dinstein, Textural features for image classification, IEEE Trans. Syst. Man Cybern (1973) 610-621.

[2] R.F. Walker, P.T. Jackway, D. Longstaff, Genetic algorithm optimization of adaptive multi-scale GLCM features, Int. J. Pattern Recognition Artif. Intell. (2003) 17-39.

[3] D.C. He, L. Wang, Texture unit, texture spectrum and texture analysis, IEEE Trans. Geosci. Remote Sensing (1990) 509-512.

[4] D.C. He, L. Wang, Texture features based on texture spectrum, Pattern Recognition (1991) 391-399.

[5] D.C. He, L. Wang, Unsupervised textural classification of images using the texture spectrum, Pattern Recognition (1992) 247-255.

[6] D.C. He, L. Wang, Detecting texture edges from images, Pattern Recognition (1992) 595-600.

[7] D.C. He, L. Wang, Textural filters based on the texture spectrum, Pattern Recognition (1991) 1187-1195.

[8] C.H. Chen, L.F. Pau, P.S.P. Wang, Handbook of pattern recognition and computer vision, Word Scientific, 2000.

[9] J.R. Jensen, Introductory Digital Image Processing: A Remote Sensing Perspective, Prentice Hall, 2005.

[10] A. Barcelo, E. Montseny, P. Sobrevilla, Fuzzy texture unit and fuzzy texture spectrum for texture characterization, Fuzzy Sets and Systems (2007) 239-252.

[11] C.I. Chang, Y. Chen, Gradient texture unit coding for texture analysis, Optical Engineering (2004) 1891-1903.

[12] L. Wang, Vector choice in the texture spectrum approach, Int. J. Remote Sensing (1994) 3823-3829.

[13] P. Brodatz, Texture – a photographic album for artists and designers, Reinhold, 1968.

[14] D. Marr, E. Hildreth, Theory of edge detection, in: Proc. R. Soc., London, 1980, pp. 187-217.